NUMERICAL SIMULATION OF HELIUM LEAKAGE IN THE EXPERIMENTAL HALL AT TPS

J.C. Chang † , P.J. Wen, S.P. Kao, M.C. Lin
National Synchrotron Radiation Research Center, Hsinchu, Taiwan

Abstract

To utilize helium for experiments efficiently, our beamline people built a helium recovery system at the experimental hall of Taiwan Photon Source (TPS). This system includes four helium recovery balloons, each with a capacity of approximately 13.8 m^3, and is equipped with pressure relief valves. Considering the potential safety hazard of oxygen deficit in the vicinity when helium leak occurs, this study applied numerical simulations to analyse the oxygen content distribution during cases of helium leak.

INTRODUCTION

The National Synchrotron Radiation Research Center (NSRRC) and the Max Planck Institute for Chemical Physics of Solids (MPI CPfS) in Germany jointly constructed the submicron soft X-ray spectroscopic beamline TPS 45, as shown in Fig. 1. Its goal is to utilize various synchrotron radiation spectroscopic techniques to reveal the electronic structure of novel strongly correlated materials. The TPS 45 beamline uses liquid helium to cool the superconductors to conduct experiments at low temperatures. However, to keep precious helium from dissipating into the atmosphere and causing unnecessary waste [1], the volatile gaseous helium produced during the cooling process is recovered and reused through four balloons, as shown in Fig. 2.

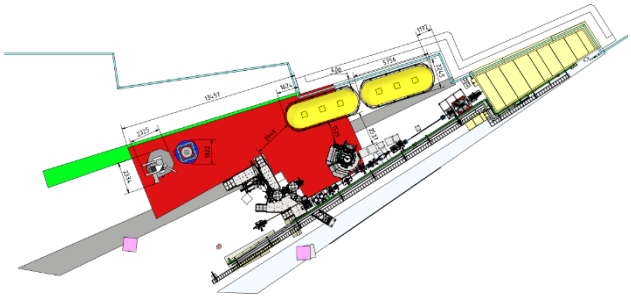

Figure 1. Top view of the TPS45 beamline.

Each experiment requires 50 liters of liquid helium. The volume of each cylindrical balloon with length of 5.5 m and diameter of 1.9 m is 13.8 m^3. However, if helium leaks from the balloons, it may cause oxygen deficiency in the area, posing a hazard to personnel conducting experiments there. Therefore, an oxygen-deficiency assessment is required to ensure personnel safety [2]. As a result, a series of simulations was conducted to estimate oxygen concentration under various helium leakage conditions [3].

The helium recovery system was set up in the TPS experimental hall. The inner and outer ring radii of the experimental hall are 87 m and 104 m, respectively, with a height of 10.5 m.

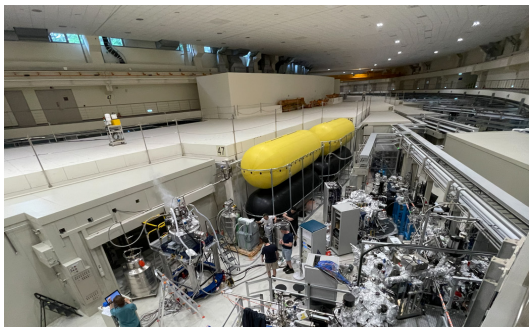

Figure 2. TPS45 helium recovery balloon.

The helium recovery system consists of four helium recovery balloons (as shown in Fig. 1). The pressure relief valve has an inner diameter of 4 cm and a pressure relief range of 20-60 mbar, which is adjustable and currently set at 50 mbar. The balloons can continuously supply pressure up to 500 mbar, and the flow rate is controllable. This study focuses on numerical simulation analysis of helium leakage in this system. To conserve memory, we model a 1/12 segment of the experimental area, within which the helium recovery system is located (as shown in Fig. 3).

NUMERICAL SIMULATION

CFD (Computational Fluid Dynamics) began from the early 30s of the 20th century to solve the linearized potential equations with 2D methods. As rapid development of numerical analysis and computer science, CFD has been widely applied in many fields. In this study, we perform the CFD to simulate helium leakage in the experimental hall of TPS.

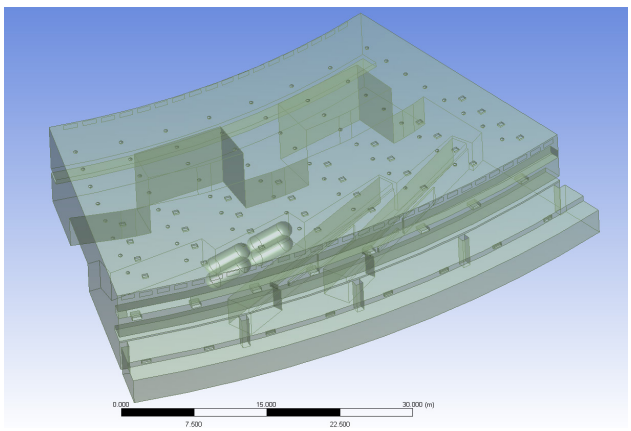

Figure 3: 3D schematic view of one twelfth of the TPS experimental hall.

We performed CFD of 3D numerical simulation using a commercial code Fluent R.16.2. [4]. To save computing

memory and time, we simulate one twelfth of the TPS experimental hall, as shown in Fig. 3. In this study, we generate a horizontal and a cross section virtual planes H and V, respectively to exam the simulation results. The height of plane H is 1.5 m.

Governing Equation

The basic governing equations include the continuity equation, the momentum equation and the energy equation.

We apply the k-ε turbulence model and SIMPLEC to solve the velocity and pressure problem.

Mass conservation equation (continuity equation)

$$\frac{\partial \rho}{\partial t} + \nabla \cdot (\rho \mathbf{u}) = 0 \tag{1}$$

where ρ is density of fluid (air in the study), t is time and $\mathbf{u}$ refers to air velocity vector.

Momentum conservation equation

$$\frac{\partial (\rho \mathbf{u})}{\partial t} + \nabla \cdot (\rho \mathbf{u}\mathbf{u}) = -\nabla p + \rho \mathbf{g} + \nabla \cdot (\mu \nabla \mathbf{u}) - \nabla \cdot \tau_t \tag{2}$$

where p is pressure, $\mathbf{g}$ is vector of gravitational acceleration, μ is dynamic viscosity of air, and τ_t is divergence of the turbulent stresses which accounts for auxiliary stress due to velocity fluctuations.

Energy conservation equation

$$\frac{\partial (\rho e)}{\partial t} + \nabla \cdot ((\rho e + p)\mathbf{u}) = \nabla \cdot \left(k \nabla T - \sum_j h_j \mathbf{j}_j \right) \tag{3}$$

where e is the specific internal energy, T is air temperature, k is heat conductivity, h is the specific enthalpy of fluid, $\mathbf{j}$ is the mass flux.

Geometry and Grid Generation

We set a detailed 3D model of one twelfth of experimental hall of TPS for the numerical simulation. The height of this space is 10.7m. The space of the simulation zone is about 12,313 m^3.

In this model, the heat sources include lights, distributed on the ceiling, daylight windows, distributed on the top areas of walls of the inner and outer rings as shown in yellow, two beamlines and some equipment.

According to the geometry of the model, we applied hybrid grid to discretize the model. The total number of the grid elements was about 6.7 million.

Boundary Conditions

There are 64 supplied air exits and 8 air exhausts distributed on the ceiling and the outer ring, respectively. Each air exit is circular with 0.2 m in diameter. Each air exhaust is a rectangular with 0.4m x 1m in size. The boundary conditions are set according to actual conditions. The air exit velocity is 2 m/s normal to the ceiling. The air exit temperature is 20 ºC. Air exhausts are set as outflow.

The four helium balloons have 4 cm orifices located at the bottom of the balloons, with a leakage pressure of 50 mbar.

RESULTS AND DISCUSSION

Figure 4 shows the distribution of oxygen mole concentration on Plane H two minutes after a helium leak at 50mbar pressure. The figure shows that the oxygen concentration near the helium balloons has dropped to as low as 12%.

Because the leak valve is located on the lower surface of the four helium balloons, most of the helium is blocked by the beam at a height of 1.5 meters, preventing it from flowing upwards and allowing it to flow only downwards. The gradient of oxygen concentration distribution can be observed in the contour diagram. The oxygen concentration at the bottom of the figure is approximately 19%, while the concentration at the top and left remains at 21%.

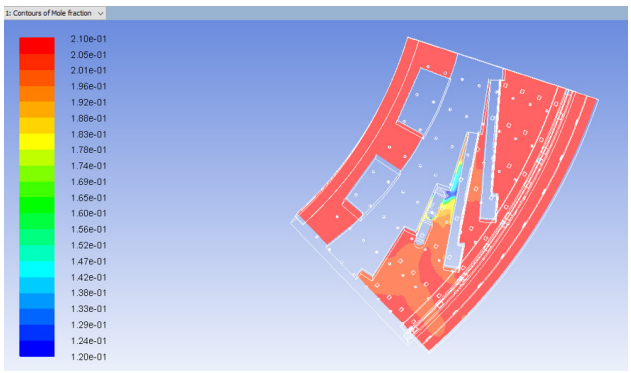

Figure 4: Simulated distribution of oxygen mole concentration on Plane H after two minutes helium leak at 50 mbar pressure.

Figure 5 shows the distribution of oxygen moiré concentration on Plane V two minutes after a helium leak at 50 mbar pressure. The same as Fig. 4, where the oxygen concentration near the helium balloons is as low as 12%.

Although the leak valve is located on the lower surface of the four helium balloons, there are no obstructions above the balloons, and due to the low density of helium, helium can flow freely upwards to the ceiling. Although the supplied air exits of the AC system are located on the ceiling, the oxygen concentration in most of the space above is below 19%, especially below 17% directly above the helium balloons. The lower left portion of the space still maintains 21%, consistent with Fig. 1.

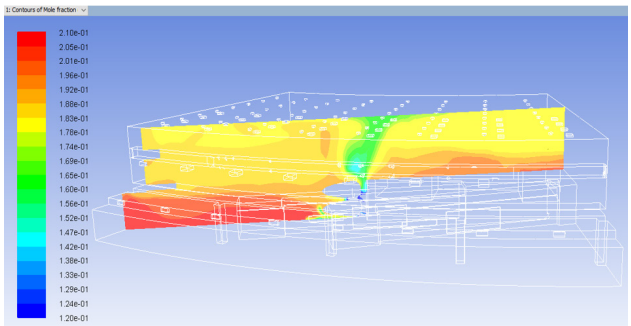

Figure 5: Simulated distribution of oxygen mole concentration on Plane V after two minutes helium leak at 50 mbar pressure.

Figure 6 shows the pathlines from the supplied air exits and the helium leak. The figure shows that the oxygen concentration in the supplied air flowing out of the air exits is 21%. However, the oxygen concentration in the supply air near the helium leak drops rapidly and disperses in all directions. On the other hand, the oxygen concentration in the supply air further away from the helium leak drops more slowly and vertically flows downwards. The oxygen concentration at the helium outlet is 0.

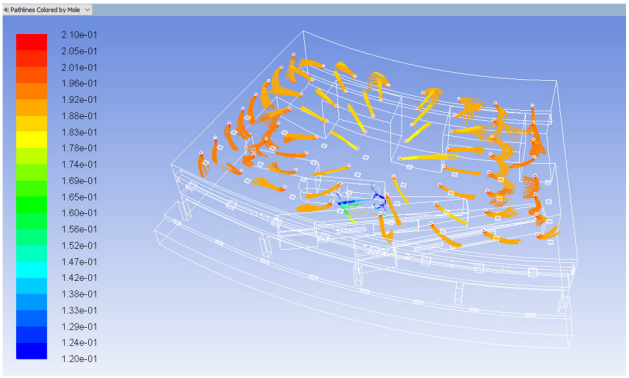

Figure 6: Pathlines from the supplied air exits and the helium leak.

We set up eight observation points at four locations near the helium leak, at heights of 0.6 meters and 1.2 meters, as shown in Fig. 7.

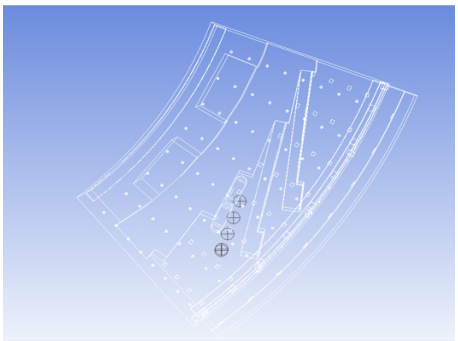

Figure 7: Four virtual locations near the helium leak.

Figure 8 shows the variations in oxygen concentration at these eight observation points and the average oxygen concentration at plane H (h =1.5 m) over five minutes.

The figure shows that the oxygen concentration at points P1-0.6, P1-1.2, and P2-0.6, closest to the helium leak, dropped sharply within one to two seconds after the leak, followed by a rapid increase in oxygen concentration due to the downward leakage of helium. This phenomenon was not observed at points P2-1.2, plane H, and P3 and P4, slightly further away, but the oxygen concentration still decreased over time. The oxygen concentration changes at the four observation points at 0.6 meters and 1.2 meters of P3 and P4 were very similar, dropping below 20% approximately four minutes after the leak and still remaining at 19% after five minutes.

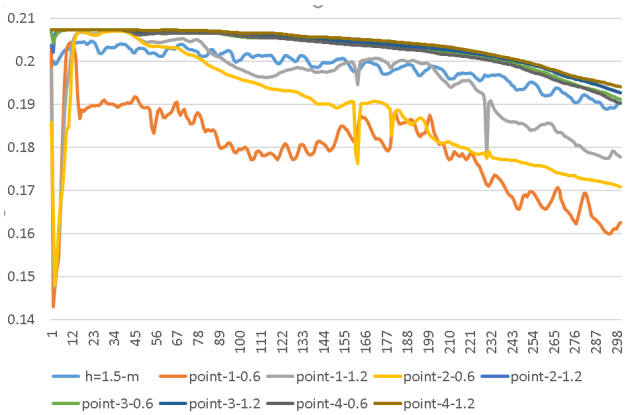

Figure 8: Variations in oxygen concentration at these eight observation points and the average oxygen concentration at plane H (h =1.5 m) over five minutes.

CONCLUSION

We used numerical simulations to show the changes in oxygen concentration in the vicinity after a helium leak. This study provides our colleagues with information of how oxygen concentration in the experimental area decreases over time in the event of a helium leak.

ACKNOWLEDGEMENT

Authors would like to thank colleagues in the TPS 45 of NSRRC for their assistance.

REFERENCES

[1] L Dufay-Chanat *et al.*, “Final report on the Controlled Cold Helium Spill Test in the LHC tunnel at CERN”, *OP Conf. Ser.: Mater. Sci. Eng.* Vol. 101, p. 012123, 2015. doi:10.1088/1757-899X/101/1/012123

[2] R. Andersson *et al.*, “Numerical simulation of cold helium safety discharge into a long relief line”, *Physics Procedia*, Vol. 67, pp. 1112-1116, 2015. doi:10.1016/j.phpro.2015.06.172.

[3] J.-C. Chang *et al.,* “Experimental Validated CFD Analysis on Helium Discharge”, in *Proc. MEDSI'16*, Barcelona, Spain, Sep. 2016, pp. 156-158. doi:10.18429/JACoW-MEDSI2016-TUPE02

[4] ANSYS. Fluent product documentation.